Measurement Characterization for Localizing Multiple RFI Sources Simultaneously from a UAS

Adrien Perkins, *Stanford University*
Sherman Lo, *Stanford University*
J David Powell, *Stanford University*

BIOGRAPHIES

Adrien Perkins is a Ph.D. candidate in the GPS Research Laboratory at Stanford University working under the guidance of Professor Per Enge in the Department of Aeronautics and Astronautics. He received his Bachelor of Science in Mechanical Aerospace Engineering from Rutgers University in 2013 and his Master of Science in Aeronautics and Astronautics from Stanford University in 2015.

Sherman Lo is a senior research engineer at the Stanford University GPS Laboratory.

ABSTRACT

To combat the threat posed by jammers, a UAS based system has been developed to be able to rapidly localize the source of GPS interferers. Previously, the focus of the project, an unmanned aerial system (UAS) known as JAGER, has been on the development of a system capable of localizing a single static radio frequency interference (RFI) source [1]. JAGER is a UAS comprised of three main systems: the sensor to measure the bearing to the interference source, the localization system responsible for estimating the source location, and a path planning system to fly the vehicle in a way to minimize the cost of localization (typically thought of as the time to localize a source within a threshold) [2]. This works presents an analysis of the capabilities of the sensor, a phased array antenna, in an environment with multiple RFI sources. Understanding the sensor capabilities is key to being able to choose the right approach for localization and path planning.

The introduction of additional interference sources poses a key challenge on the sensor's ability to detect and measure the bearing to multiple sources simultaneously from a single receive signal strength (RSS) pattern. This paper presents a characterization and theoretical analysis of the performance of a 3-, 7-, and 19-element array in an environment with multiple interference sources. The difference in beamwidths of the different array sizes and side lobe suppression result in biases in the bearing measurements for the smaller arrays, while the larger arrays come at additional size, weight, and monetary costs, creating a set of tradeoffs to be considered for a system to localize multiple RFI sources from a UAS. To detect multiple sources, JAGER uses an onboard beam steering antenna to generate an RSS pattern (by measuring signal strength). For each RSS pattern, the bearing to each of the lobes detected is determined using the 3dB method used for bearing determination to a single source [3]. The theoretical performance of this method is evaluated in two different simulated multi-source environments. Finally, some design constraints are presented for the bearing sensor for detecting multiple sources based on the desired angular separation capabilities.

INTRODUCTION

JAGER has been designed to be able to rapidly localize a single static interference source (e.g. a PPD) using a 3-element phased array antenna. The technique used to determine the bearing to the signal source is to make a collection of signal strength measurements by steering the antenna to different azimuth angles to create an RSS pattern. From that RSS pattern, a bearing observation can be extracted given the directionality of the antenna.

Localizing signal sources requires three key systems onboard JAGER: a sensor to make measurements to the source(s), a localization algorithm to estimate the location of the source(s), and a path planning algorithm to fly the UAS in the best direction in real time to minimize the cost of localization (typically thought of as the time to localize source(s) within a threshold). The path planning method is highly dependent on the localization approach and the sensor characteristics and is considered to be beyond the scope of this paper.

The task of localizing multiple targets, whether moving or static, is a very active topic of research, with a wealth of different algorithms having been designed [4]. The core challenge of multi-source is the ability to associate the measurement with one of the estimated sources. Due to this, multisource localization algorithms tend to fall into one of three categories: joint probability data association (JPDA), multi-hypothesis tracking (MHT), and random finite set (RFS) based methods [4]. Within each of these categories, algorithms have been developed to improve certain characteristics of the algorithm, such as methods for handling bearing-only measurements or methods for handling environments with large amounts of clutter [5]. Despite all the differences between these algorithms, they all depend on an understanding of the sensor and the resulting measurements. For all these approaches they key factor is understanding the error characteristics of the measurements which include both any biases the sensor might have and the probability of measurements that do not associate with any true source, known as clutter. For this reason, this paper focuses on characterizing the sensor and the measurements from three different sized antenna arrays: a 3-, 7-, and 19-element phased array antenna.

The characterization of the performance is broken down into three factor: the maximum theoretical sensor error which is broken down into error caused by biases due to the antenna shape and biases due to the incident angle of the RFI source(s), the maximum range of the sensor which is computed as relative ranges between the different sensors instead of absolute range, and finally the amount of cluttered measurements.

The detection analysis compares 3 different antenna arrays: a 3-, 7-, and 19-element array on a hexagonal grid with a half wavelength spacing, as shown in Figure 1. A hexagonal grid layout is used so that the resulting pattern has circular symmetry making it ideal for generating RSS patterns to detect bearing to signal source(s) [6]. The antennas are modeled using the phased array toolbox in Matlab.

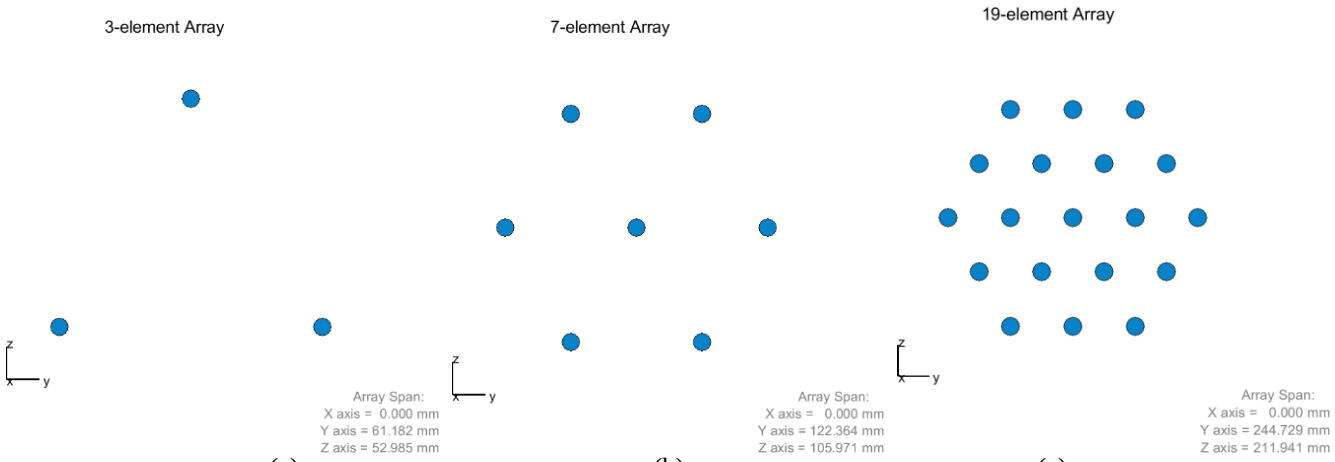

Figure 1: Element layout for hexagonal grid arrays of (a) 3 elements, (b) 7 elements, and (c) 19 elements

Frames of Reference

Throughout this paper the dominant frame, when discussing the antenna pattern and signal directions, is a spherical coordinate system with angles ϕ and θ. The angle ϕ is defined as the angle from the Y axis towards the X axis and is defined on [0, 360) – this is the same as the definition for heading in an NED frame. The angle θ is defined as the angle from the Z axis towards the XY plane. For this project, the antenna axis is defined to have the Z axis normal to the antenna elements. Furthermore, the antenna is mounted upside down on the vehicle and the X axis of the frame is aligned with the East axis of an NED frame, effectively lining up the antenna's XYZ axis to the vehicle's local horizontal NED frame. This means that the angle θ is the angle from vertically down towards the horizon (θ=0° points straight down and θ=90° points to the horizon).

Organization

The organization of the paper is as follows. The first section (Sensor Characterization) characterizes the expected performance of three different sized antenna arrays for observing bearing to two interference sources. The characterization focuses on the theoretical accuracy of each array size given multiple interference sources and the effects of distortion when steering an array. The second section (Bearing Observation) demonstrates the capabilities, and limitations, of the 3dB method of bearing

extraction from a multisource RSS pattern in a simulated environment containing 2 equal powered sources. Finally, the last two sections present some concluding remarks relating the simulation results to necessary design choices for the localization algorithm and path planning and present future areas of development for successful simultaneous localization.

SENSOR CHARACTERIZATION

This section focuses on characterizing the theoretical performance of each array size due to the array geometry itself. As the number of elements in the array increases the resulting pattern has a narrower beamwidth and has greater side lobe suppression when being steered. These two traits greatly affect the resulting RSS pattern when being steered. This section will first present some patterns for cases of a single source with these arrays and then will present the theoretical patterns for several illustrative two source cases. All the RSS patterns shown in this section as a result of steering the antenna to $\theta_{steer} = 60\,°$ and $\phi_{steer} = [0, 360]$ in one-degree intervals and measuring the received signal strength due to the signals present.

Single Source Pattern

The number of elements and geometry of a phased array antenna greatly impact the shape of the resulting RSS patterns when being steered. For a simple 3-element array, the steered pattern will take on one of the shapes in Figure 2. For example, for $\phi_{source} = 0°$ the resulting pattern will have one main lobe and 2 side lobes as depicted in Figure 2a. For $\phi_{source} = 90°$ the result will have one main lobe and one prominent back lobe, as depicted in Figure 2c. Finally, for some ϕ_{source} between those angles, the result is a partially distorted pattern that typically has one sizeable back lobes and a small side lobe in addition to the main lobe, seen in Figure 2b.

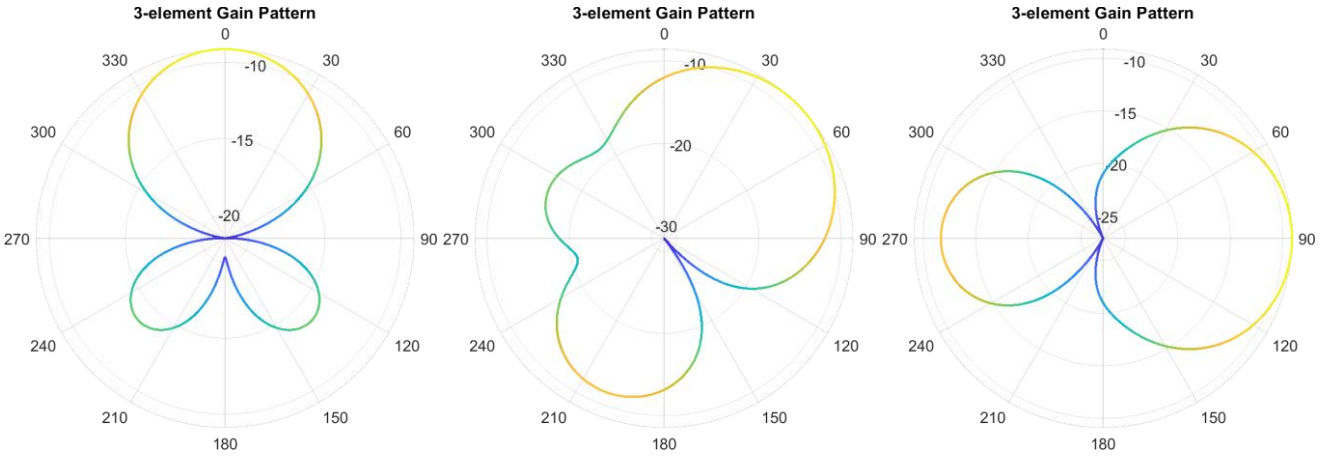

Figure 2: RSS pattern created from steering a 3-element array for a source at (a) ϕ=0°, (b) ϕ=45°, and (c) ϕ=90°

For the larger arrays there are more distinct possible choices for the patterns. The more interesting property to highlight is the side lobe suppression of the larger arrays. Taking the example of ϕ_{source} = 0°, the resulting RSS patterns for all three array sizes to the same source are depicted in Figure 3. Here it cam be see that the 3-element array, shown in 3a, are ~5dB below the main lobe, while the 7- and 19-element arrays have side lobes that are 15dB and 18dB below the main lobe, depicted in Figure 3b and Figure 3c. In addition to the improved size lobe suppression of the larger arrays (and beamwidth reduction), there is also an increase in the gain, which will result in a larger range for the larger arrays.

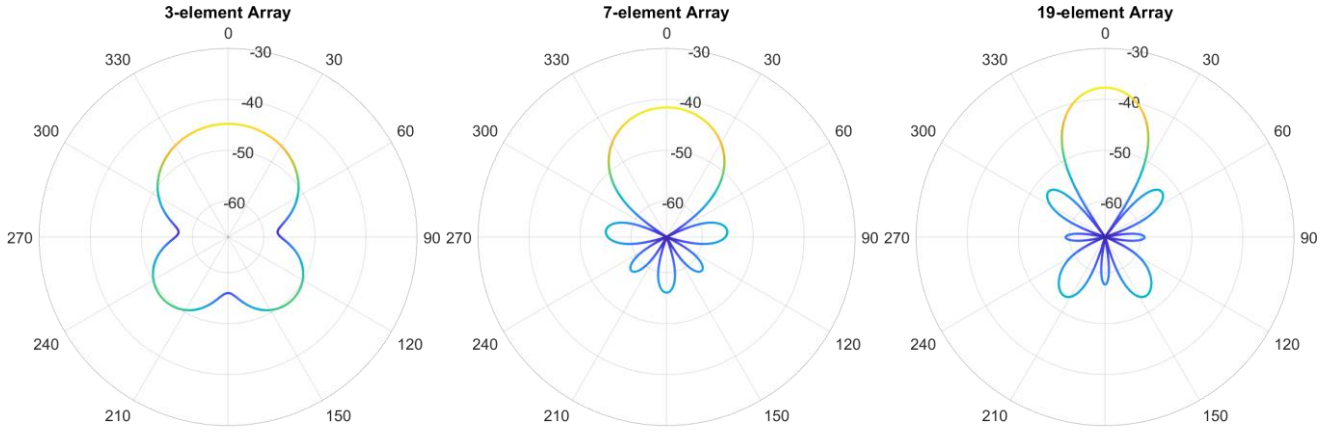

Figure 3: RSS pattern created from steering a (a) 3- element, (b) 7-element, and (c) 19-element array for a source at ϕ=0°

Multi-source Pattern

While the large side lobes of the 3-element array can be properly accounted for when there is only a single interference source, the side lobes can have large effects on the resulting RSS pattern when multiple interference sources are present, creating biases in the lobe directions depending on ϕ_{source}. This affect is illustrated in Figure 4 which shows the resulting RSS pattern from having two interference sources at $(\phi_1, \phi_2) = (0°, 90°)$. Due to the large side lobes for the 3-element array, the resulting lobes in the pattern does not point at $(\hat{\phi}_1, \hat{\phi}_2) = (0°, 90°)$, but rather at $(\hat{\phi}_1, \hat{\phi}_2) = (45°, 120°)$. Regardless of how well we can extract bearing from the RSS pattern, there is a bias due to the distortion of the pattern that needs to be resolved either through using models of the theoretical antenna performance or larger arrays. While the bias is large for some incident angles, the 3-element array can also return an RSS pattern with no bias illustrated in Figure 5 when the sources are incident at $(\phi_1, \phi_2) = (90°, 270°)$.

As the number of element in the array increase, the main lobe narrows and the side lobes are further suppressed, helping reduce the distortion in the pattern. Returning to the situation with

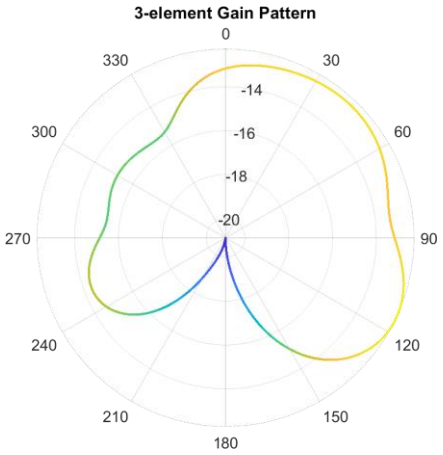

Figure 4: 3-element RSS pattern for sources at (ϕ_1, ϕ_2) = (0°, 90°)

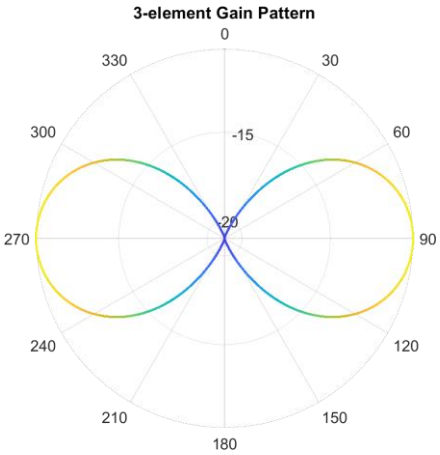

Figure 5: 3-element RSS pattern for sources at (ϕ_1, ϕ_2) = (90°, 270°)

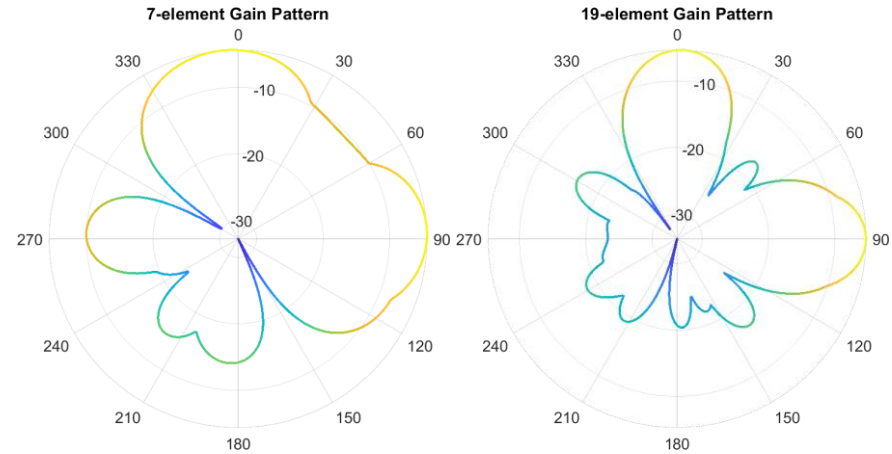

(a) (b)

Figure 6: RSS patterns for (a) 7-element and (b) 19-element arrays for sources at (ϕ_1, ϕ_2) = (0°, 90°)

2 sources at (ϕ_1, ϕ_2) = (0°, 90°), the resulting pattern for the 7- and 19-element arrays are depicted in Figure 6. The side lobe suppression of the 7-element array is already enough to remove all bias. The 19-element array, having a much smaller beamwidth, creates a set of even more defined lobes pointed in the direction of the sources and does not have any significantly large side lobes.

The RSS pattern from an array can also result in biases when the sources are angularly close to each other. Specifically when $(\phi_1 - \phi_2) > 2 * BW$, where ϕ_1 and ϕ_2 are the incident angles of the two sources in the ϕ direction and BW is the beamwidth of the steered antenna. When the sources are that close to each other, and have the same power level, the main lobe blends together, resulting in one larger main lobe pointed about half way between the two sources. Figure 7 illustrates this case for (ϕ_1, ϕ_2) = (0°, 40°) for the (a) 3-, (b) 7-, and (c) 19-element arrays. The 40 degree angular separation is less than 2*BW for all three arrays so all of the arrays have distorted main lobes with a central peak around 20 degrees. It is worth noting that the 19-element array also begins to highlight another challenge which is the apparent 3-lobe affect. Visually it can appear that there are 3 different peaks, two of which point towards the sources and a third pointing between the two. However, the ability to detect this as a single or as three peaks is a function of the bearing extraction method, discussed in the next section.

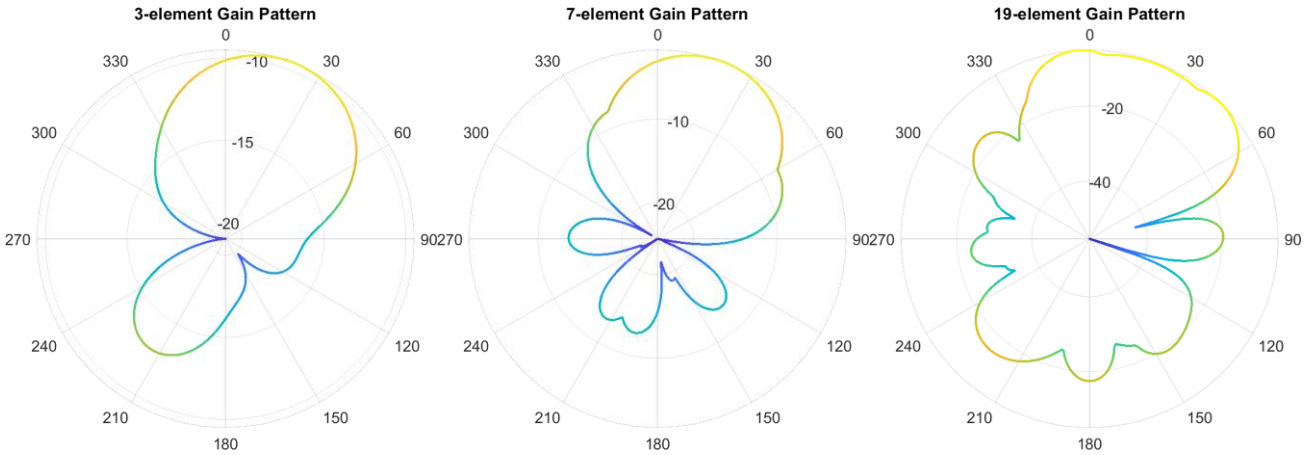

Figure 7: RSS patterns for (a) 3-element, (b) 7-element, and (c) 19-element arrays with sources at (ϕ_1, ϕ_2) = (0°, 40°)

BEARING OBSERVATION

Throughout the section the method used to determine the bearing from a given RSS pattern measurement is the 3dB method developed previously [3]. This method has been previously demonstrated to outperform other methods, such as cross correlation and max due to being agnostic to the nominal beamwidth (CC is effectively beamwidth dependent) and due to its robustness to noise in the signal strength measurements that make up the RSS pattern [7] [3]. For a quick recap of the method, to capture the effect of the shape of the RSS pattern, points on the pattern that are 3dB below the max value (shown as the gray 'x' marks in Figure 8) are used as the edges of the lobe and the bearing is taken to be the average value of those angles.

To evaluate the effectiveness and abilities of the different antenna array sizes, a 3km*3km world was simulated with two difference sets of source locations (discussed separately in Source Set A and Source Set B). The metrics used for comparison are the ability to resolve a bearing to each single source, the number of clutter measurements (bearings that do not point to a valid source), and the error of the bearing measurement due to the bias of the antenna. For this evaluation, a bearing was considered to be associated to a source if the error was less than 20°. In each simulation, the sources have the same power levels (1W) and the same

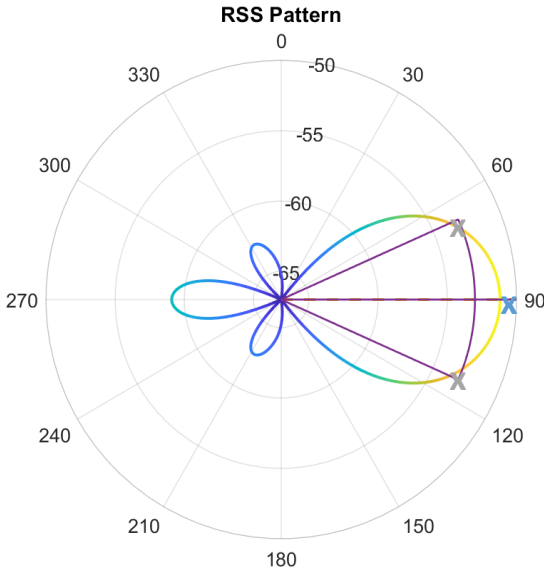

Figure 8: depiction of the 3dB method for bearing determination from an RSS pattern. The blue 'x' represents the max of the gain pattern and the gray 'x' represent the points 3dB below the max

antenna gain (2dBi). The only losses accounted for in the simulation are freespace path losses. A theoretical model of each the 3-, 7- and 19-element array is rotated at 50 meters intervals over the entire world. For each position the antenna is held at a constant altitude of 100 meters and the antenna is steered to $\theta_{steer} = 60\,°$ and $\phi_{steer} = [0, 360]$ in one-degree intervals.

Source Set A

For the first analysis, the world has two sources placed at (0, -400m) and (0, 400m). This source placement ensures that the sources go out of range of the antenna before they reach the $(\phi_1 - \phi_2) < 2 * BW$ threshold. In the second source configuration that will not be the case, enabling the comparison of these effects.

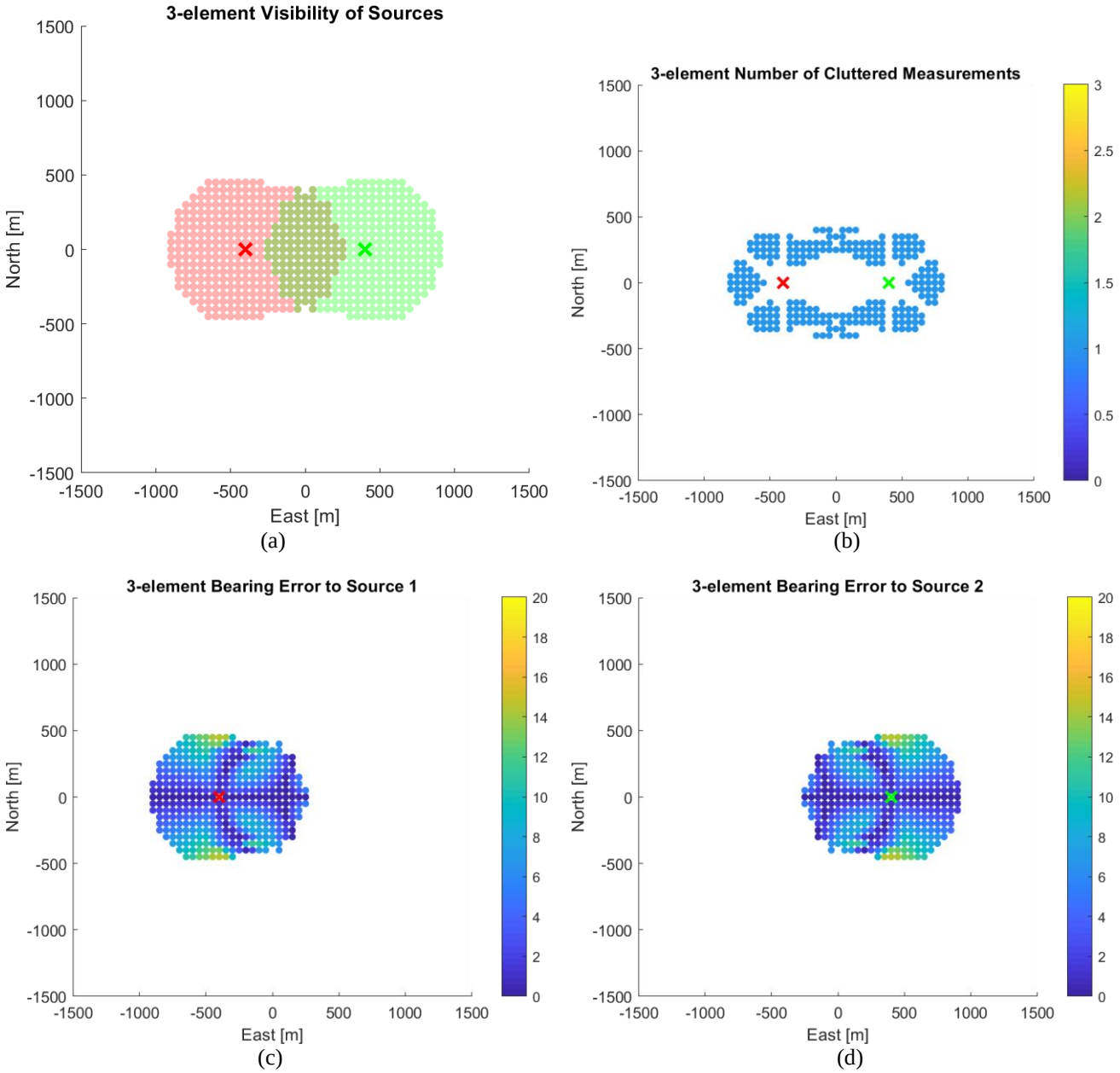

Figure 9: Bearing simulation results for a 3-element antenna with 2 interference sources at (0, -400m) and (0, 400m) showing: (a) the ability to observe a bearing to each source, (b) the number of bearing observations categorized as clutter, and (c) an

Figure 9 illustrates all of the results for the 3-element array. Figure 9a shows the visibility of each source from each location; Figure 9b shows the number of clutter observations, or bearing measurements that associated with neither source (i.e. a side lobe large enough to be detected as a main lobe); and Figure 9c and Figure 9d show the bearing error in the extracted bearing as a result of a bias in the pattern.

Immediately it can be seen that the 3-element antenna results in a lot of cluttered measurements due to the very large side lobes of the RSS pattern. Furthermore, those large side lobes also cause biases in the bearing results which are depicted in Figure 9c and Figure 9d. These biases result in errors that are up to 15° before the source becomes out of range of the sensor. Another notable result is the fact that the overlapping region does not maintain a circular shape that would be expected since the only loss considered is the freespace path loss. This is as a result of the fact that as one signal source becomes strong enough, the lobe to the weaker signal drops below the 3dB threshold of the maximum signal strength received causing it to not be detected, illustrated in Figure 10. In this example, only the larger lobe is selected as a possible bearing and the smaller lobe is missed.

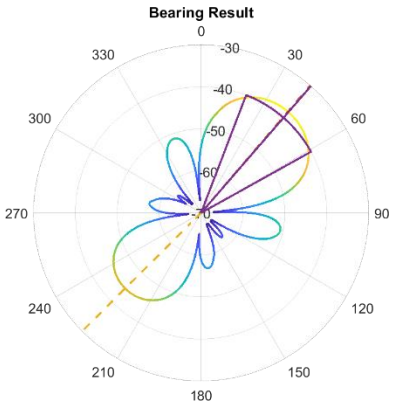

Figure 10: RSS pattern and bearing result demonstrating missed detection of weaker signal

The same results for the 7-element array are shown in Figure 12.

Immediately it is seen that, for the 7-element array, there are no clutter measurements at any location on the grid. As was seen previously, the 7-element side lobe suppression is much greater than that for the 3-element array resulting in much smaller side lobes in the created RSS patterns leading to the significant reduction in the number of clutter measurements. Looking back to the requirements for a localization algorithm and the challenges of data association, increasing the array size from 3 to 7 can greatly affect the overall performance due to the reduced amount of clutter. The smaller side lobes also reduce the distortion of the pattern and bias in the bearing measurements such that the worst case error in the RSS patterns bearings is less than 5°. However, it can also be seen that the region of overlap, where both of the sources can be seen, is also significantly reduced. Since the 7-element array has a higher gain than the 3-element array, the range to the source before the weaker signal is no longer detectable is reduced, resulting in fewer measurement locations that can provide information to both sources. Finally, as expected, the higher gain of the 7-element array results in a larger range of visibility of each of the sources.

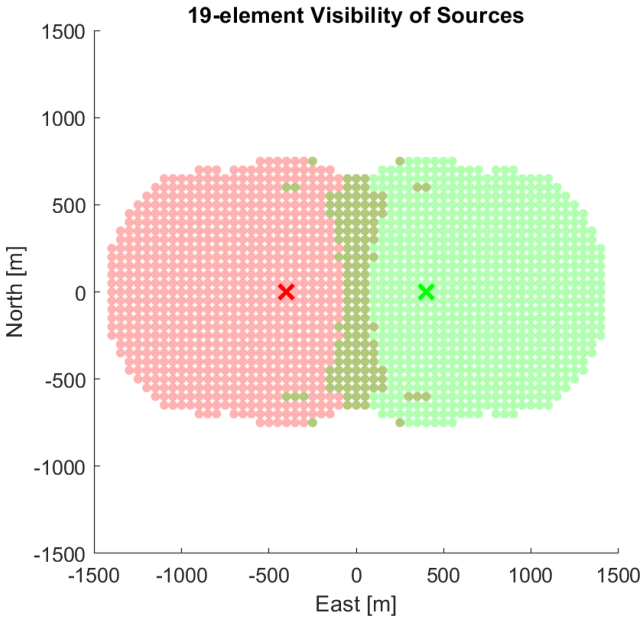

Figure 11: Visibility of each source using a 19-element array with sources at (0, -400m) and (0, 400m)

The 19-element array maintains very similar error performance as the 7-element array with the main difference being the additional range provided due to the higher gain, seen in Figure 11, showing the visible signals from the antenna.

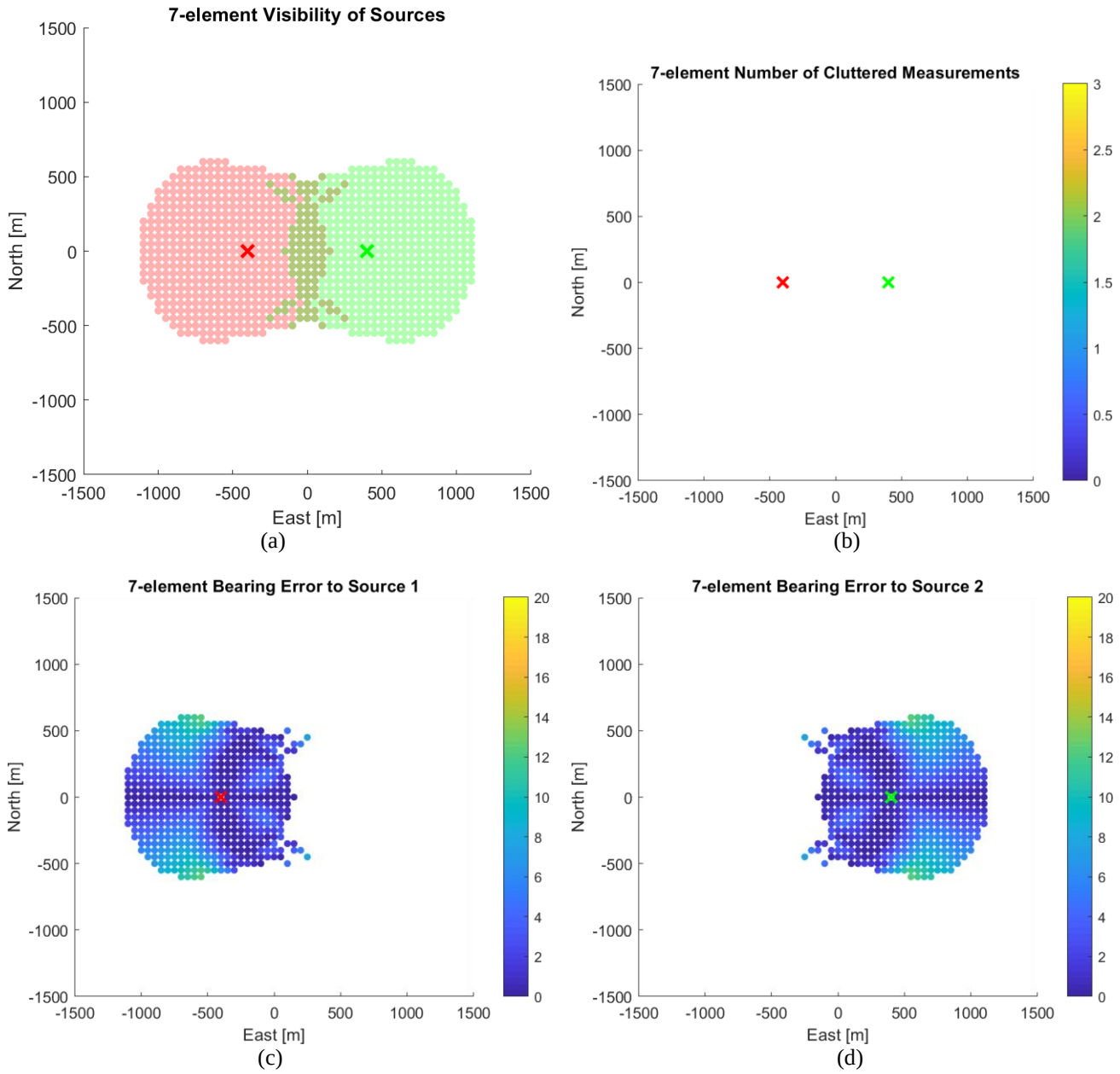

Figure 12: Bearing simulation results for a 7-element antenna with 2 interference sources at (0, -400m) and (0, 400m) showing: (a) the ability to observe a bearing to each source, (b) the number of bearing observations categorized as clutter, and (c) and (d) the observed bearing error for each source

Source Set B

For the second scenario considered, the sources are placed at (0, -200m) and (0, 200m). The placement is such that, within the range of the sensor, the angular separation of the two sources will be within the 2*BW limit to illustrate the resulting performance.

Once again rotations were simulated throughout the world with each the 3-, 7-, and 19-element arrays. The results are presented in the same format, with **Error! Reference source not found.** showing the results from the 3-element array and Figure 16 showing the results from the 7-element array.

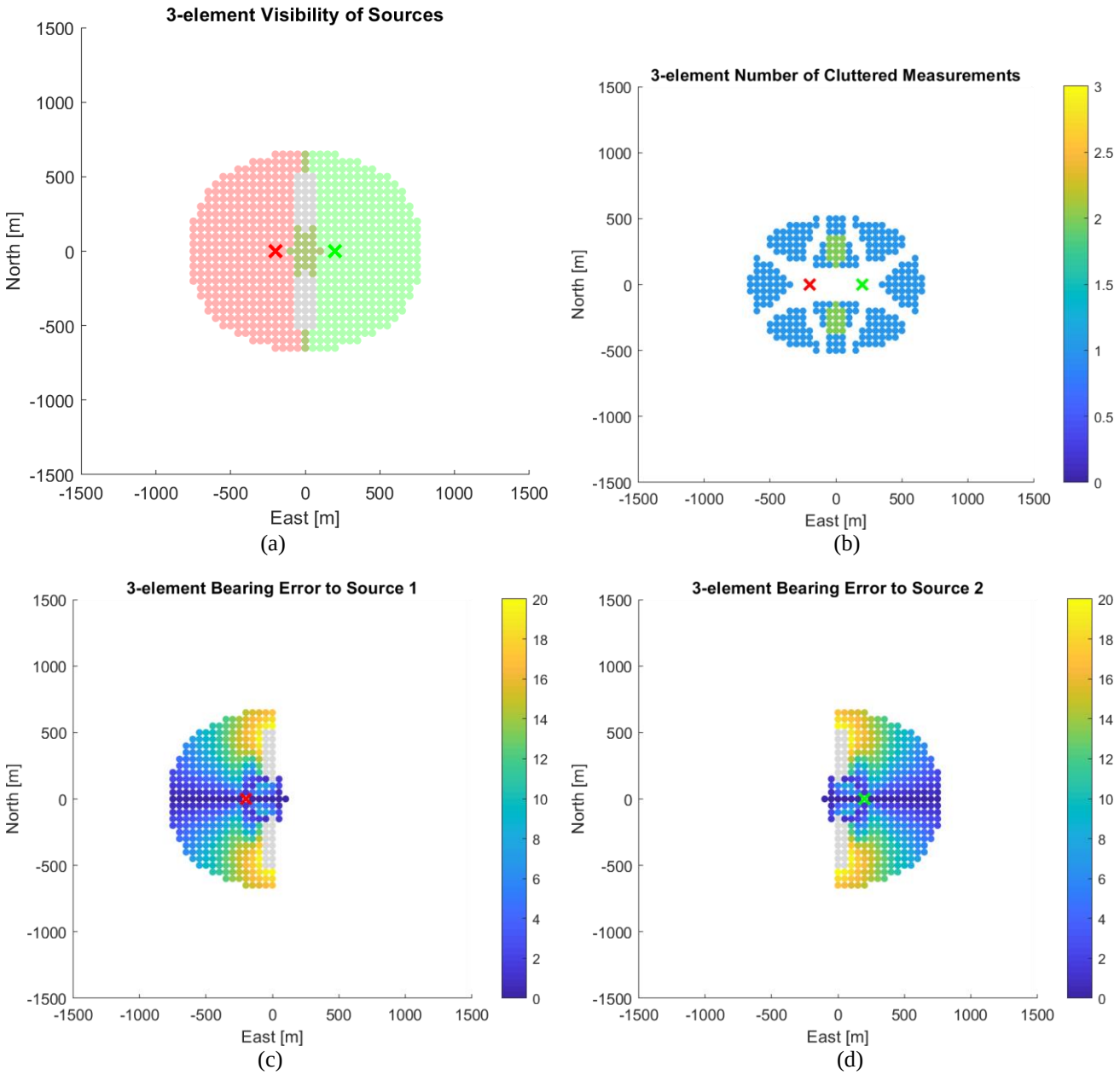

Figure 13: Bearing simulation results for a 3-element antenna with 2 interference sources at (0, -200m) and (0, 200m) showing: (a) the ability to observe a bearing to each source, (b) the number of bearing observations categorized as clutter, and (c) and (d) the observed bearing error for each source

Looking at the results for the 3-element array in Figure 13, the effects of the angular proximity of the sources is immediately apparent in the visibility plot for each source (Figure 13a) as there is a region in the center that previously has overlapping measurement that is now marked in gray and only seen in the clutter. The gray marking indicates that a bearing was seen, but did not meet the error threshold for association and therefore is not considered to associate with either source and is only clutter. For these simulations a bearing error of greater than 20° was considered to not be associated with the source, which is why those measurement now appear in clutter and not in the visibility plot. An RSS pattern in this region looks similar to the RSS pattern depicted in Figure 14 where the main lobe is stretch and the bearing is estimated to be the midpoint of the two different sources.

The second notable result is the interesting pattern in the clutter due to the distortion of the pattern is very similar to the pattern seen in the Source Set A results. This again just accentuates the difference in the RSS pattern given the incident angle of the source with some directions resulting in larger side lobes than other. This eventually can potentially be integrated into the flight controller to rotate the antenna in such a way that the signal source is incident on the antenna in a direction that minimizes clutter.

Finally of note is the much larger errors in the calculated bearing due to the biases in the board. This time the largest sources of error come in the mid region due to the inability to calculate the true bearing when the sources are angularly close to each other.

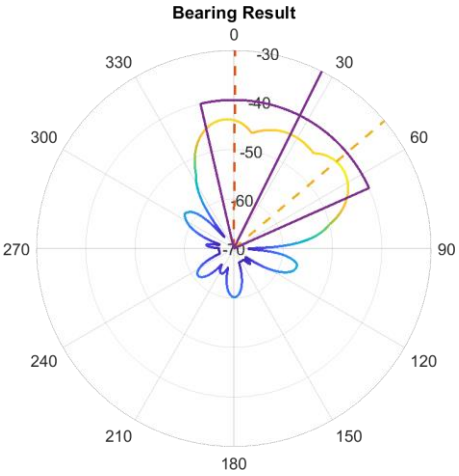

*Figure 14: Example RSS pattern for ($\phi_1 - \phi_2$) < 2*BW resulting in wrong bearing observation*

For the 7-element array, Figure 16, this source configuration does result in some clutter measurements due to the region that is affected by the sources being angularly close to each other. However, that region affected by the angular proximity is much smaller than the region for the 3-element array due to the narrower beamwidth and ability to support a smaller minimum angular separation. Just like with the 3-element array, there is an increase in the bearing error caused by the angular proximity in the sources. Once again, the 19-element array has a very similar performance as the 7-element array, with a much larger field of view, as depicted in Figure 15.

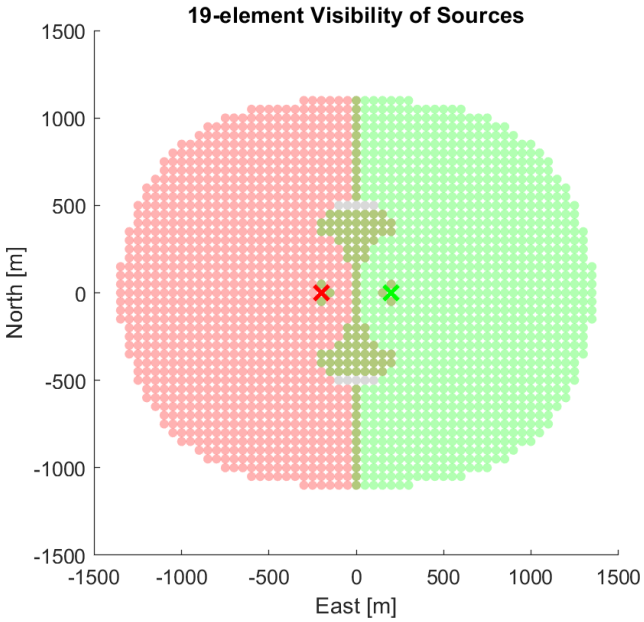

Figure 15: Visibility of each source using a 19-element array with sources at (0, -200m) and (0, 200m)

In the end there are two main sources of possible bearing error: first due to biases of the pattern due to large side lobes, and second due to sources that are angularly close to each other. While the first source of error is controllable by increasing the number of elements to a 7-element array instead of a 3-element array, the second source of error is not controllable at the sensor level. However, knowing the existence of this error source can help inform the path planning algorithm to fly in the best trajectory possible to reduce the potential of this situation occurring.

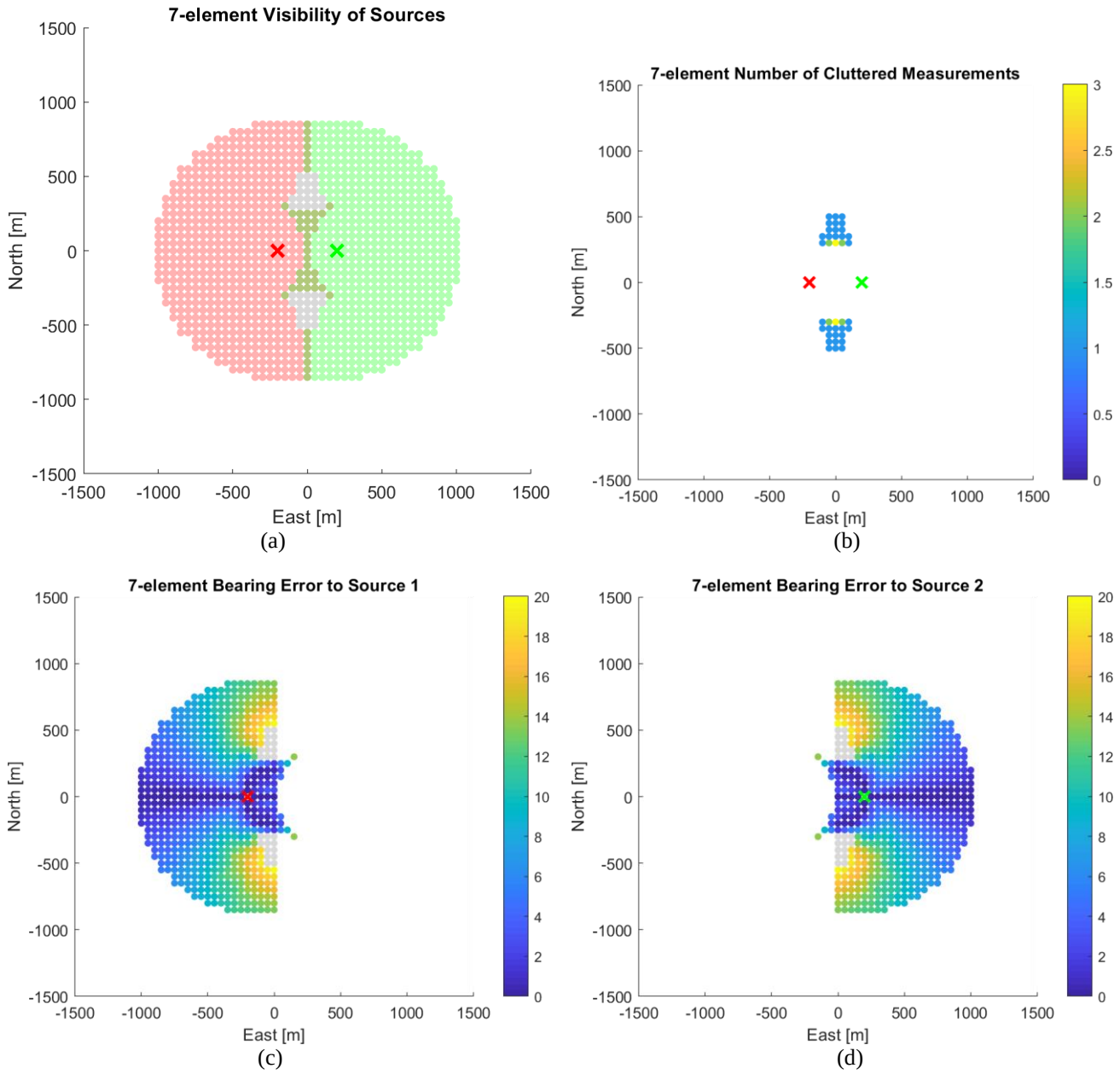

Figure 16: Bearing simulation results for a 7-element antenna with 2 interference sources at (0, -200m) and (0, 200m) showing: (a) the ability to observe a bearing to each source, (b) the number of bearing observations categorized as clutter, and (c) and (d) the observed bearing error for each source

CONCLUSION

The 3dB method is successfully able to extract bearing information from RSS patterns due to multiple RFI sources and the performance of several array sizes has been characterized and evaluated. The simulation results presented are the first step in being able to make an informed decision on the localization algorithm to use and the path planning method to use. Understanding the sensor is key to being able to get the best performance out of the sensor and get the best estimates of the RFI sources at the lowest cost (time to localization). This paper has shown that the use of a phased array antenna is still possible for a scenario with multiple RFI sources as a sensor to get bearing to the sources.

Comparing the results of the three different antennas, summarized in Table 1, some conclusions of the combined performance of the 3dB method and each array size can be made. Overall the largest design tradeoff that needs to be made is the tradeoff

between array size (weight and power) and small biases/low clutter. If using the 3-element array, the localization algorithm will need to be very robust to clutter and a good model of the sensor should be used to account for the biases that are present based on the source locations. While some biases can be addressed by cleverly choosing the flight path (e.g. flying in such a way to maintain a signal at a specific incident angle), some of the errors will need to be accounted for in the localization algorithm. Using a 7-element array comes at a cost of size, weight, but provides significant reduction of clutter and bias errors and partially reduces the "no-fly area" that would result in the sources being too angularly close to each other. The 19-element array does not provide a significant enough advantage over the 7-element array in these metrics to be worth the significant additional monetary and weight costs.

Table 1: Summary of key results from 2-source simulations for each array size

	Max Bearing Bias (far)	**Max Bearing Bias (close)**	**Min Source Angular Distance**	**Clutter**
3-element	15°	20°	150°	High
7-element	5°	20°	70°	Low
19-element	4°	20°	30°	Low

FUTURE WORK

All of the analysis so far is only steering the ϕ angle on the antenna, not the θ angle. That is an entire other dimension that is potentially useable in order to be able to modify the pattern to be able to get the best bearing observation possible. Furthermore, this discussion has been in relation to beam steering the array; another possibility is to null steer the antenna. Null steering suffers from the difficulty of having the equivalent to a very narrow beamwidth making the need to align both (ϕ_{steer}, θ_{steer}) very important in order for the source to be observable by the array. Null steering is therefore a method that can be used in the later portion of the flight, once reasonable estimates of RFI source locations are achieved and able to inform the steering angles for the antenna.

With this characterization of the measurement performance, the next step is to determine the best localization algorithm for this platform and perform test in both simulation and in the real world with multiple interference sources.

REFERENCES

[1] A. Perkins, L. Dressel, S. Lo, T. Reid, K. Gunning, and P. Enge, "Demonstration of UAV-Based GPS jammer localization during a live interference exercise," in *29th International Technical Meeting of the Satellite Division of the Institute of Navigation, ION GNSS 2016*, 2016, vol. 5.

[2] A. Perkins, Y.-H. Chen, W. Lee, S. Lo, and P. Enge, "Development of a three-element beam steering antenna for bearing determination onboard a UAV capable of GNSS RFI localization," in *30th International Technical Meeting of the Satellite Division of the Institute of Navigation, ION GNSS 2017*, 2017, vol. 4.

[3] A. Perkins, L. Dressel, S. Lo, and P. Enge, "Antenna characterization for UAV based GPS Jammer localization," in *28th International Technical Meeting of the Satellite Division of the Institute of Navigation, ION GNSS 2015*, 2015, vol. 3.

[4] R. P. S. Mahler, *Statistical Multisource-Multitarget*. 2007.

[5] Q. Zhang and T. L. Song, "Improved Bearings-Only Multi-Target Tracking with GM-PHD Filtering.," *Sensors (Basel).*, vol. 16, no. 9, Sep. 2016.

[6] H. L. Van Trees, "Planar Arrays and Apertures," in *Optimum Array Processing*, New York, USA: John Wiley & Sons, Inc., 2002, pp. 231–331.

[7] J. Graefenstein, A. Albert, P. Biber, and A. Schilling, "Wireless node localization based on RSSI using a rotating antenna on a mobile robot," in *2009 6th Workshop on Positioning, Navigation and Communication*, 2009, pp. 253–259.